Water Science & Technology



Water Science & Technology Vol 87 No 4, 866 doi: 10.2166/wst.2023.024

# Treating mechanical washing wastewater with iron-in-oil characteristics by changing the fate of iron

Jinyi Qin [a,b,*], Yiwen He[a], Botao Shangguan[a], Ruiqi Wang[a], Xing Wang[b], Chuan Qin[c] and Yu Wang[d]

[a] School of Civil Engineering, Chang'an University, Xi'an 710054, China
[b] Shaanxi Keeping Environmental Sci-Tech Co., Ltd, Xi'an 712000, China
[c] Shaanxi Environmental Protection Oil and Gas Engineering Co. Ltd, Xi'an 710065, China
[d] SWAG Water Affair Science & Technology Research Center, Xi'an 710004, China
*Corresponding author. E-mail: jinyi.qin@chd.edu.cn

JQ, 0000-0001-5727-1846

## ABSTRACT

The mechanical washing wastewater contained a large amount of oil, and the iron wrapped in the oil was slowly released into water. This caused the effluent quality to fluctuate, causing common polymeric aluminum chloride (PAC) to ineffectively remove the water-in-oil. The method uses $Ca^{2+}$ to demulsify and $ClO_x^-$ to destroy the water-in-oil structure, which releases Fe from the oil droplets. The active oxygen produced by $NaClO_x$ further converts $Fe^{2+}$ into $Fe^{3+}$ and then combines with NaOH to form $Fe(OH)_3$-flocs core, which improves the flocculation efficiency of PAC. The optimal ratio was approximately 400 μL of $NaClO_x$, 200 μL of 1 mol $L^{-1}$ CaO, and 12 mL of 12.8 g $L^{-1}$ PAC. The oil removal rate reached 99.88% and the residue density was 178.42 mg $L^{-1}$. The maximum Fe and chemical oxygen demand (COD) removal rates were close to 49.2 and 99.89%, respectively. In field applications, wastewater should be acidified first, and acidification oxidation is more effective than direct oxidation. In short, a novel way for treating mechanically washed wastewater with iron-in-oil characteristics by changing the environmental fate of iron is provided.

**Key words:** coagulation–flocculation, fate of Fe, mechanical washing wastewater, $NaClO_x$, water-in-oil structure

## HIGHLIGHTS

- 49.2% of Fe and 99.89% of COD were removed by $NaClO_x$ + CaO + PAC.
- The optimal ratio was 400 μL of $NaClO_x$, 200 μL of 1 mol $L^{-1}$ CaO, and 12 mL of 12.8 g $L^{-1}$ PAC.
- $NaClO_x$ destroys the water-in-oil and alters the environmental fate of Fe to $Fe(OH)_3$ for promoting flocculation.
- Acidification prior to $NaClO_x$ oxidation benefits the removal of COD and iron.

## GRAPHICAL ABSTRACT

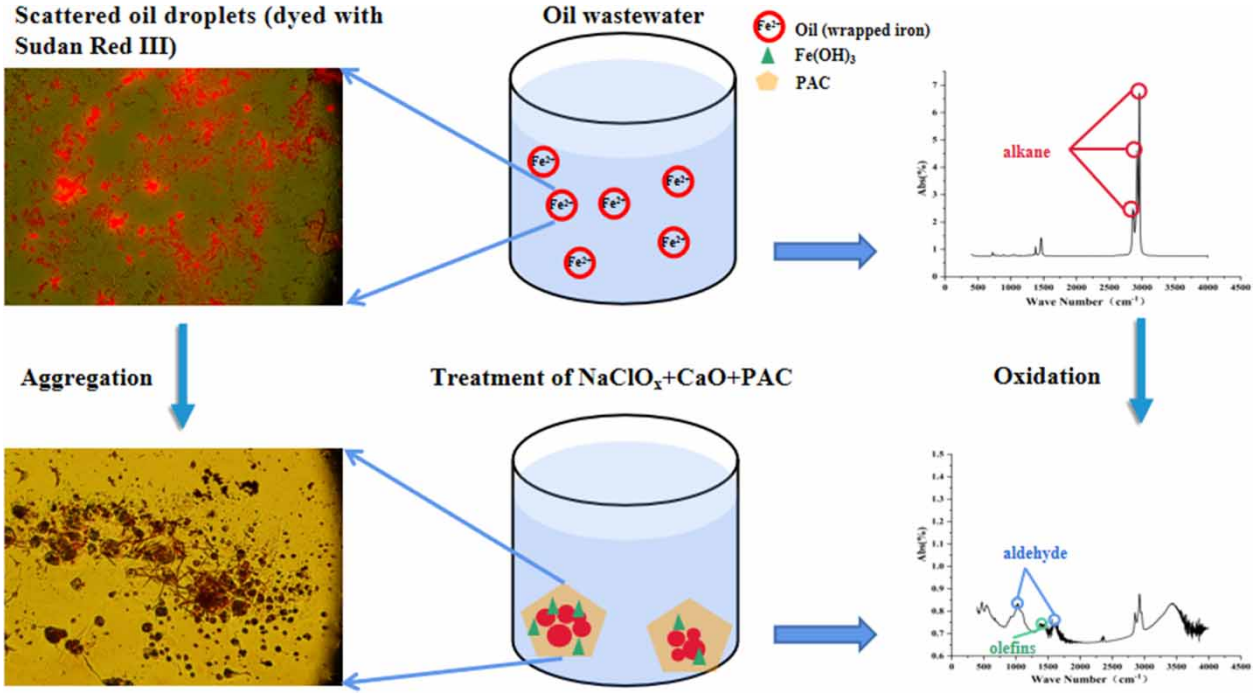


## 1. INTRODUCTION

Machinery wastewater is primarily derived from the water used to wash machinery surfaces and the ground after maintenance. Washing wastewater contains large amounts of surfactants and oils (Liu *et al.* 2020) and is highly dispersed with a complex chemical composition containing significant amounts of iron. This composition causes challenges when treating environmental discharge (Meng *et al.* 2012). If wastewater is improperly treated and discharged into the environment, major pollution even can occur, which can endanger human health (Cao *et al.* 2018). Treatment methods include gravity separation, air flotation, membrane separation, adsorption, and flocculation (Hui *et al.* 2015; You *et al.* 2018; Han *et al.* 2019). Flocculation is an effective method for treating oil-containing wastewater (Zhao *et al.* 2008; Fard *et al.* 2016; Deghles & Kurt 2016).

Chitosan, alum, and PAC (polyaluminum chloride) have been used as coagulants to treat residual oil and suspended solids in palm oil wastewater, achieving removal rates of residual oil and suspended solids of >95% (Iskandar *et al.* 2018). The combination of zinc polysilicate and anionic polyacrylamide (A-PAM) can remove 99% of the oil and leave <5 mg $L^{-1}$ residual suspended solids when treating heavy oil wastewater (Zeng *et al.* 2007). For the coagulation and foam separation of PAC and milk casein, 95% of the water-in-oil can be removed (Zhang *et al.* 2017). Hydrogen peroxide, combined with ultraviolet rays and $TiO_2$ to oxidize wastewater, yields a 72.5% COD removal rate and a 97.1% turbidity reduction rate (Hodaifa *et al.* 2019). However, owing to its stable water-in-oil structure, conventional oxidation–flocculation is ineffective for treating emulsified oil wastewater. Therefore, another option is to use $Fe(OH)_3$ produced by oxidation to promote flocculation and effectively remove oil. However, conventional oxidation–flocculation is ineffective for the treatment of emulsified oil wastewater because of the stable water-in-oil structure.

The addition of $NaClO_x$ and CaO to oil wastewater breaks the surfactant bond between water and oil, forcing the molecules to move to the water or oil phase (Yalcinkaya *et al.* 2020). As a result, the water-in-oil structure is broken and the oil droplets gather and float to the water surface or settle. Meanwhile, the $Fe^{2+}$ encapsulated in the oil droplets is released. $NaClO_x$ generates oxygen-free radicals and oxidizes $Fe^{2+}$ to $Fe^{3+}$ (Wang *et al.* 2006). $Fe^{3+}$ reacts with hydroxyl radicals in water to form hydroxides or polyhydroxides. The surface of $Fe(OH)_3$ is mostly cationic group, which can absorb negatively charged oil droplets and pollutant particles (Cañizares *et al.* 2007; Chen *et al.* 2022). These molecules have a large surface area and their affinity for water-in-oil can be leveraged for use as an effective adsorbent to remove emulsified water-in-oil (Crespilho &

Rezende 2004). Based on adsorption, bridging and other processes, the size of $Fe(OH)_3$ increases after absorbing pollutants. As a core, $Fe(OH)_3$ forms a dot network with the organic polymer chain, which is conducive to the removal of pollutants (Zhang *et al.* 2015).

Common chemicals such as $NaClO_x$, CaO, and PAC have been produced on a large scale in the world, with high output and low price. Therefore, using them for industrial wastewater treatment has practical advantages and feasibility (Zheng *et al.* 2015; Wen *et al.* 2018; Darvishmotevalli *et al.* 2019; Ganiyu *et al.* 2020).

Herein, a novel treatment of emulsified oil wastewater, entitled demulsification–oxidation–flocculation, is proposed. The oil droplets were embedded in paraffin and used for section observations, and the FTIR characteristics of the wastewater and flocs were determined. The distribution of Fe in oil, water, and sediments was tracked and $Na^+$, $Ca^{2+}$, and $OH^-$ concentrations were determined to clarify their effects on the residual iron and oil contents as well as COD. Based on the removal effect, the optimal ratios of $NaClO_x$, PAC, and $CaCl_2$ were determined. Finally, the difference between oxidation after acidification and direct oxidation during the newly developed oil wastewater treatment was investigated. This paper provides an effective new route for the mechanical washing of wastewater using $Fe(OH)_3$-floc cores produced by oxidation and demulsification to promote the water-in-oil structure decomposition and flocculant precipitation.

## 2. MATERIALS AND METHODS

### 2.1. Materials and reagents

Washing wastewater was collected and stored at 4 °C before use. Analytically pure calcium hypochlorite, sodium hypochlorite, sodium hydroxide, polyaluminum chloride, petroleum ether, o-phenanthroline, sodium acetate, ammonium acetate, and glacial acetic acid were purchased from Sigma-Aldrich (Missouri, USA). All reagents used in the field experiments were industrial grade. The commercial active oxygen oil-removing agent AOORA-2106 (main component $NaClO_x$; $x = 1, 2, 3, 4$; hereinafter referred to as $NaClO_x$ reagent) was provided by Shaanxi Keeping Environmental Sci-Tech Co., Ltd (Xi'an, China).

### 2.2. $Ca^{2+}$, $Na^+$, and $OH^-$ effects on coagulation and flocculation

First, 150 mL of wastewater was poured into a 300 mL beaker along with 400 μL of $NaClO_x$ and 12 mL of 12.8 g $L^{-1}$ PAC. Subsequently, one of four treatments was applied: (1) 200 μL of 1 mol $L^{-1}$ CaO; (2) 200 μL of 1 mol $L^{-1}$ $CaCl_2$; (3) 200 μL of 1 mol $L^{-1}$ $Ca(OH)_2$; or (4) 200 μL of 1 mol $L^{-1}$ NaOH. The pH values of (3) and (4) were adjusted to 12. The four processed samples were subjected to centrifugation at 150 rpm for 10 s and 30 rpm for 5 min. After standing for 15 min, the supernatant and sediment were collected for further measurements.

### 2.3. FTIR measurements and paraffin-embedded-section observation for floc structure and functional group determination

The raw and treated wastewater were filtered to obtain flocs, which were then divided into two parts. One part was dried and analyzed using FITR and the other was dyed with Sudan Red III, embedded in paraffin, and sectioned for observation.

### 2.4. Dosage optimization

First, 150 mL of wastewater was removed and 4, 6, 8, 10, or 12 mL of 12.8 g $L^{-1}$ PAC were added along with 400 μL of $NaClO_x$ and 200 μL of 1 mol $L^{-1}$ CaO for Group I; 200, 250, 300, 350, and 400 μL of 1 mol $L^{-1}$ CaO were added along with 400 μL of $NaClO_x$ and 12 mL of 12.8 g $L^{-1}$ PAC for Group II; 300, 350, 400, 450, and 500 μL of $NaClO_x$ were added along with 200 μL of 1 mol $L^{-1}$ CaO and 12 mL of 12.8 g $L^{-1}$ PAC for Group III. Phenanthroline spectrophotometry (HJ T 345-2007) was used to determine the iron content in the raw water and treated supernatant. The samples were also extracted with petroleum ether for 3 h, and the oil content was measured by absorbance using an ultraviolet spectrophotometer. The COD was determined using the dichromate method (GB11914-89), and each data point was measured in triplicate.

### 2.5. On-site treatment process of oil wastewater

A schematic of the on-site treatment process of oil wastewater is shown in Figure 1. The oil wastewater entered the grease trap for preliminary oil–water separation and then flowed into the adjustment tank to complete acidification. After the wastewater was oxidized and demulsified, it was mixed with flocculants and pumped into the air flotation tank. The oil slick was removed by skimming the upper part of the tank, and the flocculated sludge was discharged from the bottom. After the effluent in the middle was biochemically treated, it reached the discharge standard and was subsequently reused.

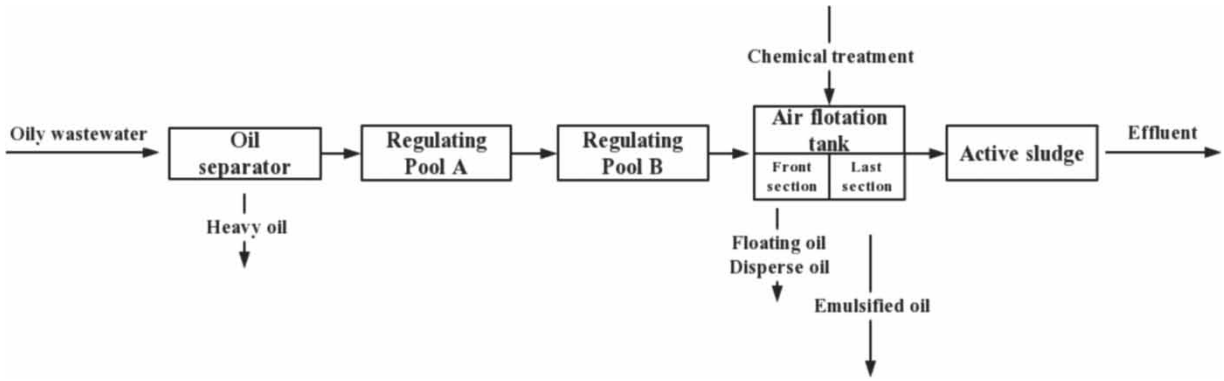


**Figure 1** | Schematic illustration of the on-site treatment process for wastewater.

### 2.6. Acidification + oxidation and direct oxidation experiments

For the acidification + oxidation samples, acid was added to adjust the pH to 6 and 400 μL of $NaClO_x$ was subsequently added after standing for 12 h. Simultaneously, an equal amount of $NaClO_x$ was added to the directly oxidized sample. The supernatant was removed every 4 h and 12 mL of PAC was added. After static sedimentation, the remaining Fe and COD concentrations in the supernatant were determined.

## 3. RESULTS AND DISCUSSION

### 3.1. Paraffin-embedded-section observation of the $Fe(OH)_3$-floc structures

As shown in Figure 2(a), the oil droplets in the original wastewater were orange-red after dyeing with widely distributed small particles in the field of view. The oil droplet area accounted for 73.48% of the view, indicating a relatively high oil content in the water. Figure 2(b) shows that flocs were produced after the addition of $NaClO_x$ + CaO. The small orange-red oil droplets were no longer dispersed and instead started to aggregate (Chen *et al.* 2022). This is mainly because $NaClO_x$ releases active oxygen-free radicals to attack the oil droplets in wastewater (Wang *et al.* 2006). The emulsified oil structure was oxidized, releasing $Fe^{2+}$ encapsulated in the oil and generating a gel suspension of Fe hydroxide or polyhydroxide (Equation (1)).

$$HClO + Fe^{2+} \rightarrow HO^{\cdot} + Fe^{3+} + C1^{-} \quad (1)$$

Under surface complexation of Fe, the oil acts as a ligand (L) to chemically combine with Fe: L + H(OH)OFe → L-OFe + $H_2O$ (Moussa *et al.* 2017). By itself, $Fe(OH)_3$ is a good flocculant that precipitates with oil by complexation or electrostatic attraction, to remove oil from water. In addition, $Ca^{2+}$ addition reduces the negative charge on the floc surface, disrupting the steady state and initiating coagulation. At this time, the area of the oil droplets accounted for 19.27% of the total view.

Figure 2(c) shows the floc structure generated by the addition of $NaClO_x$ + CaO + PAC. $Fe(OH)_3$ colloidal particles with the same charge normally repel, maintaining a stable dispersion state, and do not effectively precipitate to become effectively removed. PAC, as a polymer inorganic flocculant, imparts a significant bridging effect on $Fe(OH)_3$-oil flocs (Chaprão *et al.* 2018). Compared with the flocculation structure produced by $NaClO_x$ + CaO (Figure 2(b)) and PAC (Supplementary Figure S1), the orange-red oil droplets coalesced more tightly and the flocculated area increased to 19.64% of the total view.

Figure 2(d) shows the supernatant and its contents after $NaClO_x$ + CaO + PAC addition to oil wastewater, wherein the red oil droplets were significantly reduced compared with Figure 2(a), with the oil area accounting for only 0.8% of the total view for a removal rate of 98.92%. Except for a few red oil droplets, blue fluorescent substances were observed. In the context of the literature, it was inferred that the excess $Ca^{2+}$ and $CO_2$ gas formed $CaCO_3$ crystals, which emitted blue fluorescence under UV light (Qin *et al.* 2021). Therefore, a high-density sedimentation tank was suggested to be added at the outlet of the coagulation tank, supplementing the insoluble medium particles. In addition, seed crystals could be added to accelerate the growth of $CaCO_3$ crystals and allow $CaCO_3$ gravity sedimentation and adsorption to promote oil removal effects.

The proposed mechanism of $NaClO_x$ enhancing PAC flocculation is shown in Figure 3. $NaClO_x$ oxidized the oil droplets, released $Fe^{2+}$ wrapped in the oil, and generated Fe hydroxide. $Fe(OH)_3$ can be used as the core to enhance the formation of

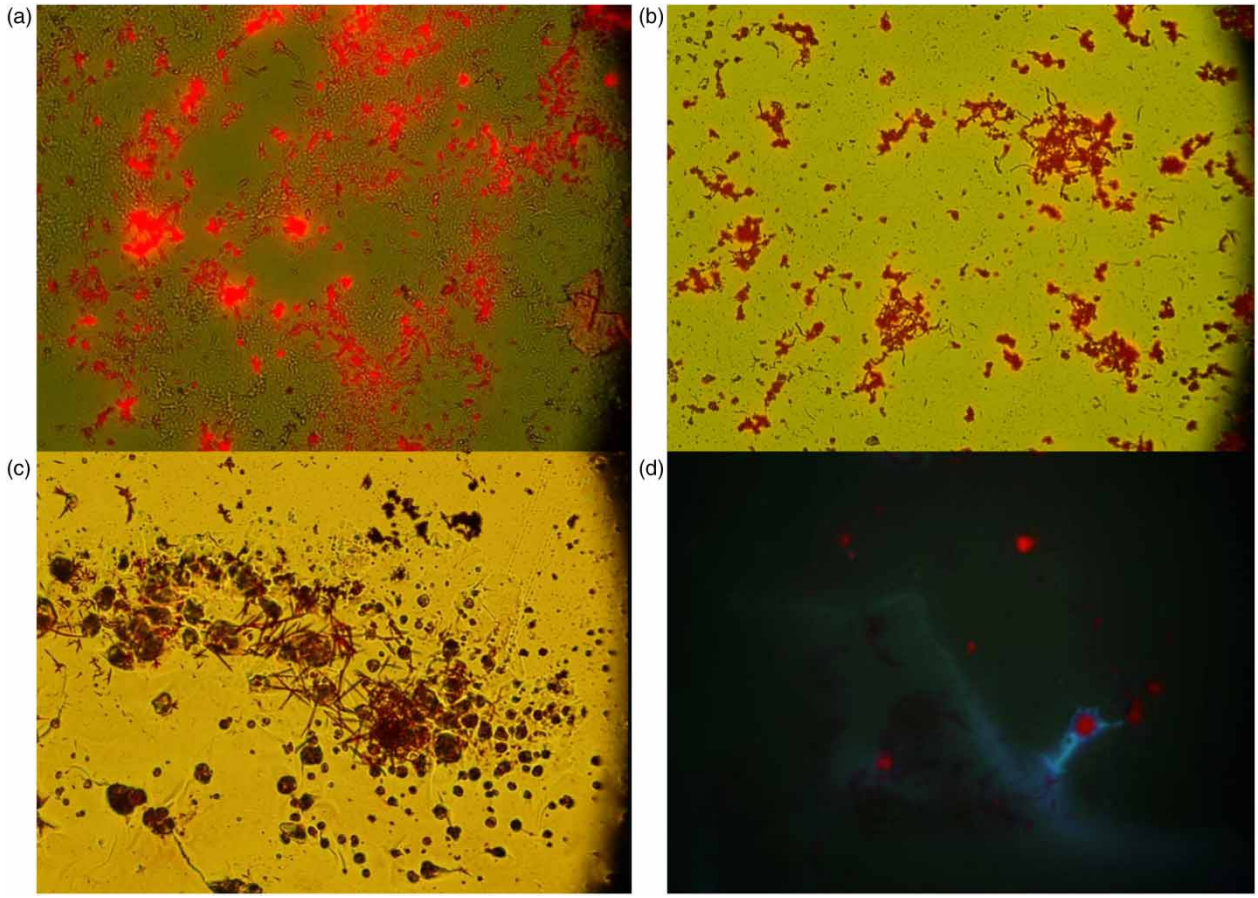


**Figure 2** | Original wastewater (a), flocs of $NaClO_x + CaO$ (b), flocs of $NaClO_x + CaO + PAC$ (c), and the $NaClO_x + CaO + PAC$ supernatant (d) observed by Sudan red staining.

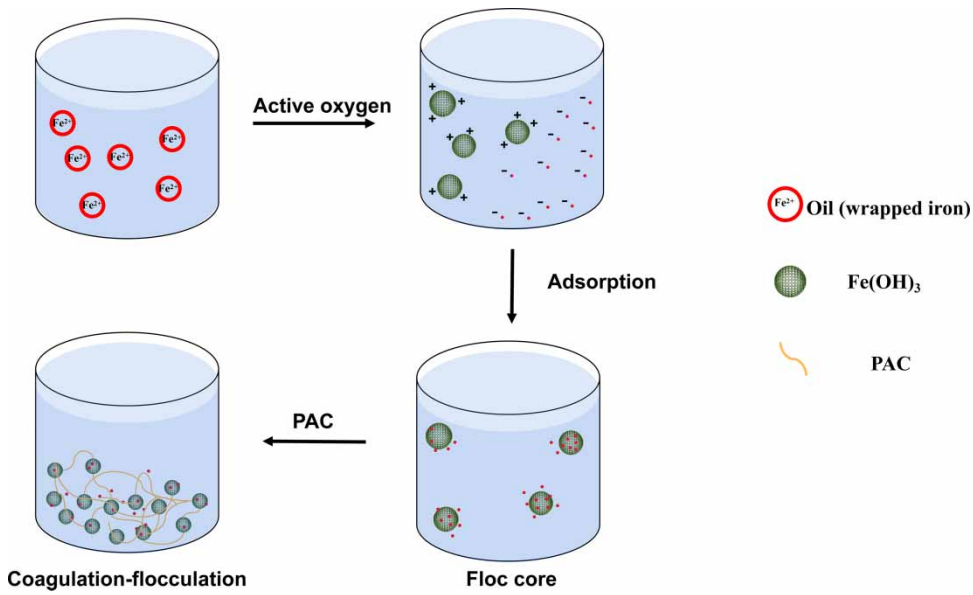


**Figure 3** | Schematic of the mechanism of nuclear flocculation.

settleable flocs with higher density, size, and strength, and increase the concentration of particles in wastewater, so that the average distance between particles was relatively short, and the electric double layer was reduced, resulting in higher collision frequency, thus removing oil droplets (Simate *et al.* 2015; Lv *et al.* 2018). Although PAC hydrolysates with organic matter cannot be removed by natural sedimentation, they can be adsorbed by $Fe(OH)_3$ to form Al species-$Fe(OH)_3$ particles cluster, whose large flocs can be removed easily (Yan *et al.* 2008; Lee *et al.* 2012; Zhang *et al.* 2017).

### 3.2. Effects of supplementing $Ca^{2+}$, $Na^{+}$, and $OH^{-}$ in wastewater on $Fe(OH)_3$ flocculation

As shown in Figure 4, the oil content of the raw water was 456.14 mg $L^{-1}$. Based on $NaClO_x$–PAC flocculation adding other reagents including NaOH, CaO, and $CaCl_2$, the remaining oil concentration reached 126.32, 156.14, and 164.91 mg $L^{-1}$, respectively, for respective oil removal rates of 72.31, 65.77, and 63.85%. In comparison, the oil removal rate after $Ca(OH)_2 + NaClO_x$–PAC treatment was significantly increased to 83.46%, and the residual oil concentration was only 75.43 mg $L^{-1}$. The main purpose of adding the other reagents is to destroy the water-in-oil emulsion structure. High ion valence generally leads to improved demulsification effects. Compared with $Na^{+}$, $Ca^{2+}$ is a more effective demulsifier, forming an oil-removing floc precipitate (Liu *et al.* 2020). In addition, the amount of heat released by the contact between CaO and water was much higher than that of $Ca(OH)_2$ (Pardo *et al.* 2014), which significantly increased the temperature of the wastewater and promoted Brownian motion of the $Fe(OH)_3$ colloidal particles. This reduced the chances of collision between $Fe(OH)_3$ and oil, thereby reducing floc production. The oil removal efficiency of CaO was shown to be inferior to that of $Ca(OH)_2$.

As mentioned in Section 3.1, after the structure of the water-in-oil emulsified layer was destroyed, the encapsulated $Fe^{2+}$ was released and oxidized by the active oxygen-free radicals released by $NaClO_x$ to form a $Fe(OH)_3$-floc core and precipitate. The Fe content of the original wastewater was 3.8 mg $L^{-1}$, whereas the residual Fe concentration after CaO treatment was 0.185 mg $L^{-1}$ for a removal rate of 95.13%. After other treatments, the remaining iron was approximately 0.2 mg $L^{-1}$, with the iron removal rate reaching 94%. Therefore, the Fe removal mechanisms of $Ca(OH)_2$, NaOH, and $CaCl_2$ were comparable, but the addition of CaO induced significantly different effects that improved the iron removal efficiency considerably. Although CaO reacted with $H_2O$ to generate $Ca(OH)_2$, it formed a passivation layer that inhibited further contact between CaO and $H_2O$, generating less $OH^{-}$ than $Ca(OH)_2$ at the same molar concentration of $Ca^{2+}$. This was to use NaOH to supplement pH to 12, and discuss whether the influence of $Ca(OH)_2$ on flocculation was determined by the increase of pH. The result is that at higher pH, the PAC flocculation effect and oil droplet removal effects diminished (Kim *et al.* 2001; Munirasu

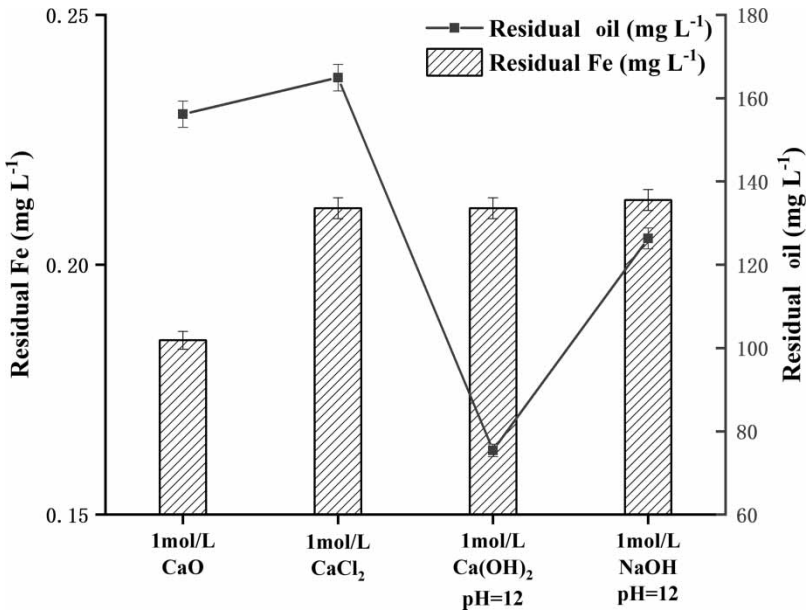


**Figure 4** | Effect of adding $Ca^{2+}$, $Na^{+}$, and $OH^{-}$ on the removal of Fe and oil in wastewater.

*et al.* 2016); thus, the former flocculation effect was better than the latter. The iron removal efficiency of CaO is significantly higher than that of $Ca(OH)_2$.

### 3.3. Functional group changes on the flocs during the oxidation–flocculation process

FTIR measurements of the functional groups in the original wastewater and the flocs after $NaClO_x$, $NaClO_x + CaO$, and $NaClO_x + CaO + PAC$ treatments are shown in Figure 5(a). The original wastewater and produced flocs exhibited three

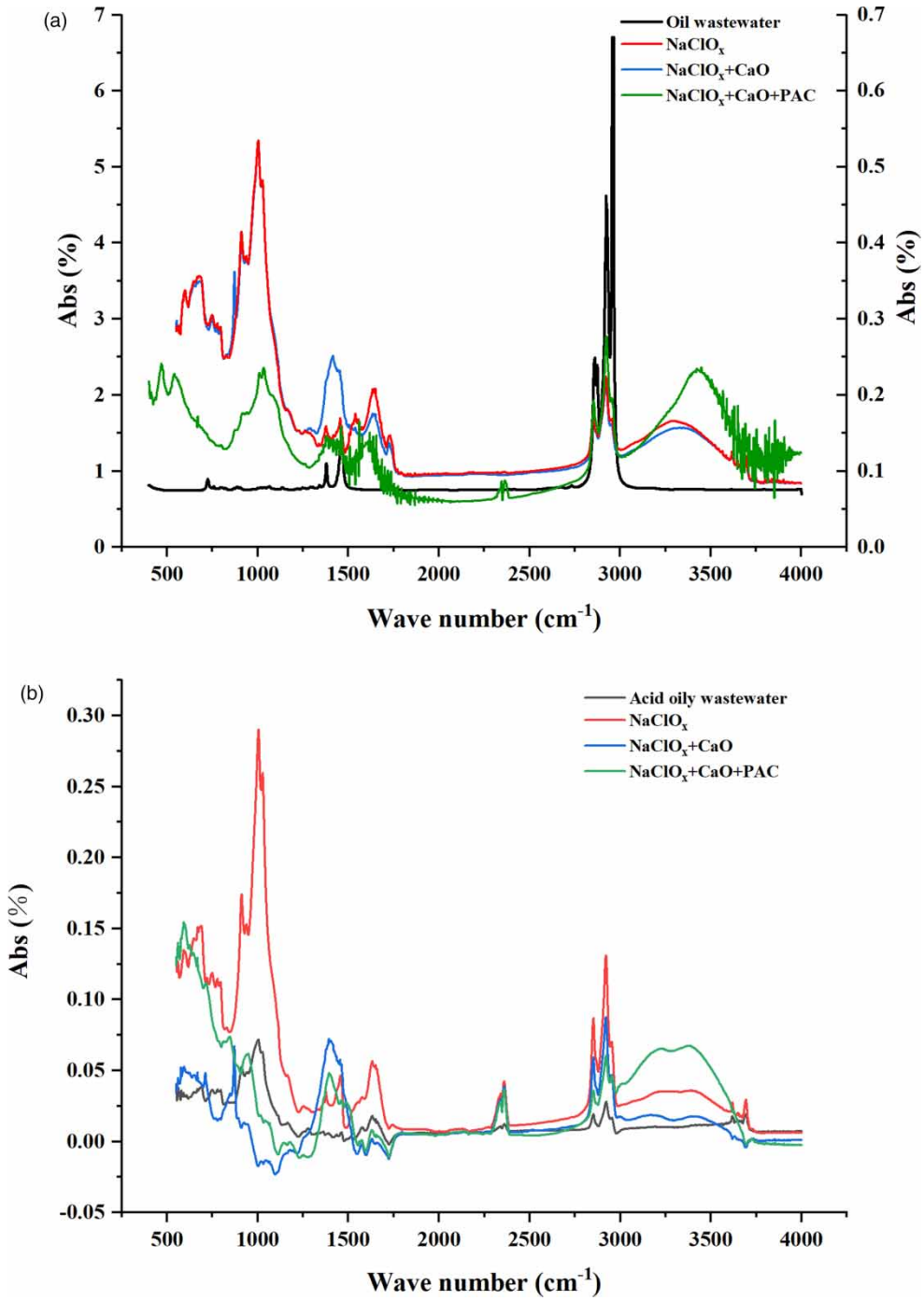


**Figure 5** | FTIR characteristics of the original wastewater (left axis) and flocs produced by $NaClO_x$, $NaClO_x + CaO$, and $NaClO_x + CaO + PAC$ (right axis) after direct oxidation (a) and acidification oxidation (b).

peaks in the 3,000–2,843 $cm^{-1}$ range. The peaks at approximately 2,960 and 2,876 $cm^{-1}$ were attributed to $RCH_3$ stretching, while those at approximately 2,930 and 2,850 $cm^{-1}$ were attributed to $R_2CH_2$. The peak at 2,890 $cm^{-1}$ was attributed to $R_3CH$, but it was rather weak (Voort *et al.* 1994). The three peaks were all saturated alkane functional groups and were most abundant in the original wastewater. Based on the intensities, the peak order is as follows: $NaClO_x + CaO + PAC > NaClO_x + CaO > NaClO_x$. Because of the high oil content in the original wastewater, a large number of hydrophobic alkane bonds were observed. After $NaClO_x$ oxidation, CaO demulsification, and PAC flocculation, the alkane groups between the oil droplets were oxidized, weakening the electrostatic repulsion. This caused the oil droplets to coagulate (Figure 2(b)), and the bulk oil was trapped and precipitated by the PAC flocs; thus, an alkane group appeared on the flocs. Compared with $NaClO_x$, $NaClO_x + CaO + PAC$ removed the oil more thoroughly, as indicated by the stronger peak response.

The R–Cl bond gave rise to a moderate absorption peak at 750–700 $cm^{-1}$ (Deng *et al.* 2016). After $NaClO_x$ was added, it reacted with alkanes to form R–Cl in the following order: $NaClO_x = NaClO_x + CaO > NaClO_x + CaO + PAC$. The three produced flocs showed an –OH intermolecular association vibration band at 3,500–3,000 $cm^{-1}$, and the peak intensity order was $NaClO_x + CaO + PAC > NaClO_x + CaO = NaClO_x$. This indicates that metal hydroxide $Fe(OH)_3$ precipitates were formed, which can serve as floc nuclei, facilitate adsorption of surrounding pollutants, and promote floc growth (Atesok *et al.* 1988). When $NaClO_x$ was added, the iron bound to the oil was released and oxidized to form hydroxide. When PAC was added, the iron hydroxide colloid settled in the flocs. Meanwhile, the halogenated hydrocarbon was also partially converted to alcohol resulting in the $NaClO_x + CaO + PAC$ treatment producing the strongest peak. This also indicated that $NaClO_x + CaO + PAC$ transformed more halogenated hydrocarbons to alcohol, explaining the low halogenated hydrocarbon peak for $NaClO_x + CaO + PAC$. The flocs showed a strong peak at 1,750–1,600 $cm^{-1}$ originating from aldehyde groups (Voort *et al.* 1994) with similar peak intensities for all three flocs. The peak at 1,200–1,000 $cm^{-1}$ arose from the out-of-plane vibration of *cis*-disubstituted olefins (Rohman & Man 2010).

As shown in Figure 6, the reaction was speculated to occur as follows. After adding $NaClO_x$, the generated unstable HClO was decomposed into HCl and $O_2$. HCl reacts with the remaining HClO to generate a small amount of $Cl_2$ in the aqueous phase, which then reacts with light alkanes to form chlorinated hydrocarbons; hence, the chlorinated hydrocarbon functional group peaks at 750–700 $cm^{-1}$. The chlorinated hydrocarbon subsequently reacts with the hydroxide radical derived from NaOH or $Ca(OH)_2$ to generate an alcohol as follows: $R–Cl + OH \rightarrow R–OH + HCl$, corresponding to the alcohol hydroxyl group at 3,500–3,000 $cm^{-1}$. Alcohol was further oxidized by sodium hypochlorite to form an aldehyde; therefore, characteristic aldehyde peaks were observed at 1,200–1,000 and 1,750–1,600 $cm^{-1}$. In addition, $Na^+$ can react with alcohols to form sodium alkoxide, which is a good nucleophilic substituent. The chlorine atom was replaced by an alkoxy group (RO–) to form an olefin and the C = C functional group was observed at 1,500–1,000 $cm^{-1}$.

As shown in Figure 5(b), the acidic wastewater also exhibited three peaks in the 3,000–2,843 $cm^{-1}$ range, corresponding to saturated alkane functional groups. However, compared with direct oxidation, the peak signal of the acidification oxidation sample was significantly weaker, indicating an improved oil removal effect. At low pH, the polar groups of the surface-active components cause sufficient electrostatic repulsive interactions to destroy the cohesion of the interfacial membrane (Wong *et al.* 2015). After acidification and oxidation, the hydrophobic bonds in water were greatly reduced, and the hydrophobic groups were directly oxidized by the acid and converted into hydrophilic aldehyde groups. However, the peak intensity

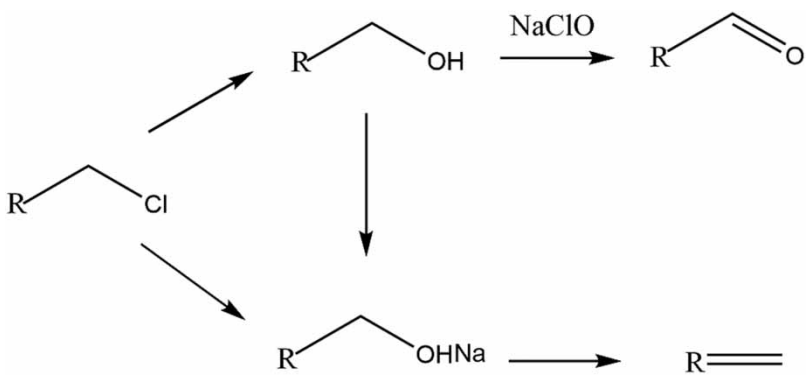


**Figure 6** | Speculative reaction during the sequential addition of NaCl, CaO, and PAC.

difference in the flocs was marginal, indicating that the change in functional groups after acidification oxidation was the same as that of direct oxidation, and the oil removal mechanism was compatible. Ultimately, acidification destroyed the water-in-oil structure.

### 3.4. Optimal ratio of $NaClO_x + CaO + PAC$ for $Fe(OH)_3$ flocculation

To determine the optimal ratio of $NaClO_x$, CaO, and PAC, the residual iron and oil contents in the supernatant after treatment were measured (Figure 7). Based on the addition of 400 μL of 10% $NaClO_x$ and 200 μmol CaO, the amounts of PAC

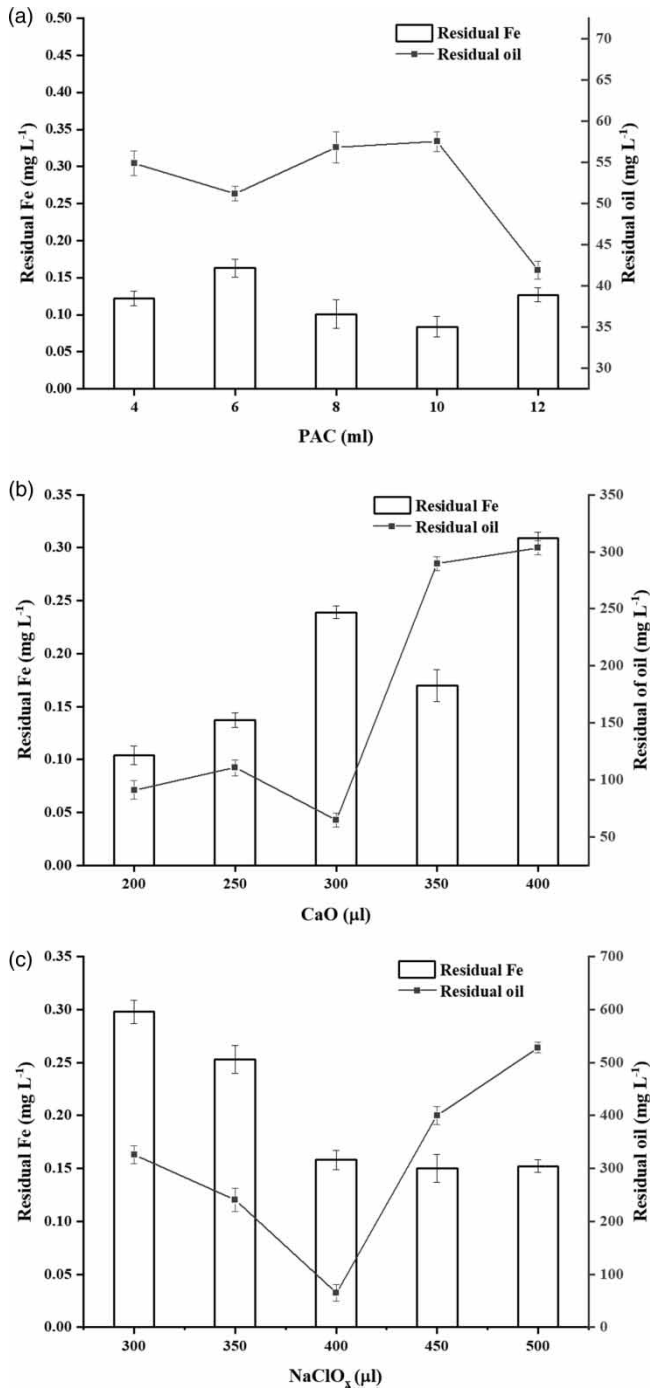


**Figure 7** | Residual Fe (column) and oil (line) in wastewater after treatment with different ratios of $NaClO_x + CaO + PAC$.

were increased. The remaining iron content in the supernatant initially decreased and subsequently increased, while the remaining iron decreased accordingly. At PAC loadings of >0.1 g, the remaining iron stabilized at 0.1 mg $L^{-1}$. However, as the addition of PAC exceeded 0.12 g, the residual Fe increased slightly. The reason for this increase was that with excessive flocculant, the produced $Fe(OH)_3$ gel was surrounded by the flocculant and was re-stabilized and settled (Xiao *et al.* 2015). Moreover, increasing PAC loadings neutralized the negative charges on the oil droplet surfaces. Dispersed oil accumulated, which is conducive to bringing it to the water surface by air flotation and skimming.

Based on the addition of 450 μL of 10% $NaClO_x$ and 0.1 g PAC, the residual iron and oil contents showed an overall upward trend with increasing CaO loading. CaO addition increased the pH and affected the flocculation efficiency of PAC. Lower pH accelerates PAC hydrolysis into positively charged polynuclear hydrolysis products $[Al_{13}(OH)_{32}]^{7+}$, which preferentially adsorb contaminant colloids and neutralize the zeta potential (Sun *et al.* 2017), conducive to coagulation. When the pH was approximately 7, $Al(OH)_3$ was the primary species involved in the sweeping mechanism. However, at a high pH, hydroxide ($OH^-$) increased the negative charge of the contaminants, which inhibited flocculation (Sillanpää *et al.* 2018). Therefore, charge neutralization or contaminant sweeping can be achieved in the presence of small amounts of CaO (approximately 200 μmol).

Based on the addition of 200 μmol CaO and 0.1 g PAC, increasing $NaClO_x$ loadings were tested, and the remaining iron initially increased and subsequently decreased, while the remaining oil content decreased and then increased. With the demulsification of $Ca^{2+}$ and oxidation of $ClO_x^-$, the water-in-oil structure was destroyed. It decomposed into slick and dispersed oil and released $Fe^{2+}$. At smaller loadings of $NaClO_x$, only the water-in-oil structure could be destroyed and continuously released $Fe^{2+}$, resulting in increased residual iron content. Here, the free water between the oil droplets was removed, which was conducive to oil coalescence and captured by the PAC. Therefore, with increasing $NaClO_x$ concentration, the amount of residual oil in the supernatant decreased. When the amount of $NaClO_x$ exceeded 400 μL, excess active oxygen-free radicals destroyed the water-in-oil structure and oxidized the released $Fe^{2+}$ into $Fe^{3+}$ precipitates. Therefore, the residual iron content in the supernatant decreased with increasing $NaClO_x$ content. However, with excess $NaClO_x$, the convergent oil was dispersed and broken into smaller oil droplets, which were more difficult to capture and remove by PAC, increasing the remaining oil content. Therefore, the best ratio for direct oxidation was determined to be 400 μL of $NaClO_x$, 200 μL of 1 mol $L^{-1}$ CaO, and 12 mL of 12.8 g $L^{-1}$ PAC.

### 3.5. Effect of acidification oxidation and direct oxidation on the removal of Fe and COD

A pilot application of 200 $m^3$ per day of mechanical washing wastewater was performed with $NaClO_x$ + CaO + PAC. The Fe and COD contents of the feed wastewater were 2.6 and 2,400 mg $L^{-1}$, respectively. The residual Fe and COD of the acidification trial were reduced to 1.42 and 1,920 mg $L^{-1}$, respectively, while those of control were reduced to 1.5 and 2,000 mg $L^{-1}$, respectively. In Figure 8(a), after acidification oxidation, both Fe and COD decreased much more than after direct oxidation, indicating that acidification accelerated the reaction process of $NaClO_x$ + CaO + PAC. This is because the low pH favors active oxygen radical generation via $NaClO_x$ (Wang *et al.* 2006), which is conducive to the destruction of water-in-oil by oxidation. Alternatively, when the wastewater pH was adjusted to acidity, an anionic surfactant, such as a high carbon fatty acid or alcohol in the emulsion, generated low carbon fatty acids, reducing hydration capability and adsorption. The interfacial tension of the surfactant and interfacial membrane strength were reduced, allowing for facile removal of the emulsion waste (Liu *et al.* 2020). Through acidification, the removal efficiencies of iron and COD were improved by 3 and 3.33%, respectively.

As shown in Figure 8(b), the removal of COD and Fe by acidification oxidation was almost linearly correlated likely because the oil layer covering Fe was acidified and hydrolyzed, while $NaClO_x$ directly destroyed the water-in-oil structure to fully contact $Fe^{2+}$. Therefore, while the COD was removed by oxidation, $Fe^{2+}$ was oxidized to $Fe^{3+}$ to form a precipitate. The fitted line for direct oxidation is parabolic. In the first 15 h, the angle was >45°, indicating that the reduction in COD was greater than that of Fe. COD removal may be related to the secondary effects of flocculation and precipitation produced by $Fe(OH)_3$. After 15 h, the fitted line stabilized and the oil was oxidized to form soluble organic matter, complicating its further capture and removal.

## 4. CONCLUSION

$Fe^{2+}$ was encapsulated in water-in-oil due to the presence of surfactants, resulting in unstable water quality of the mechanical washing wastewater. Flocculation is a technical bottleneck that cannot effectively remove oil and iron, necessitating the

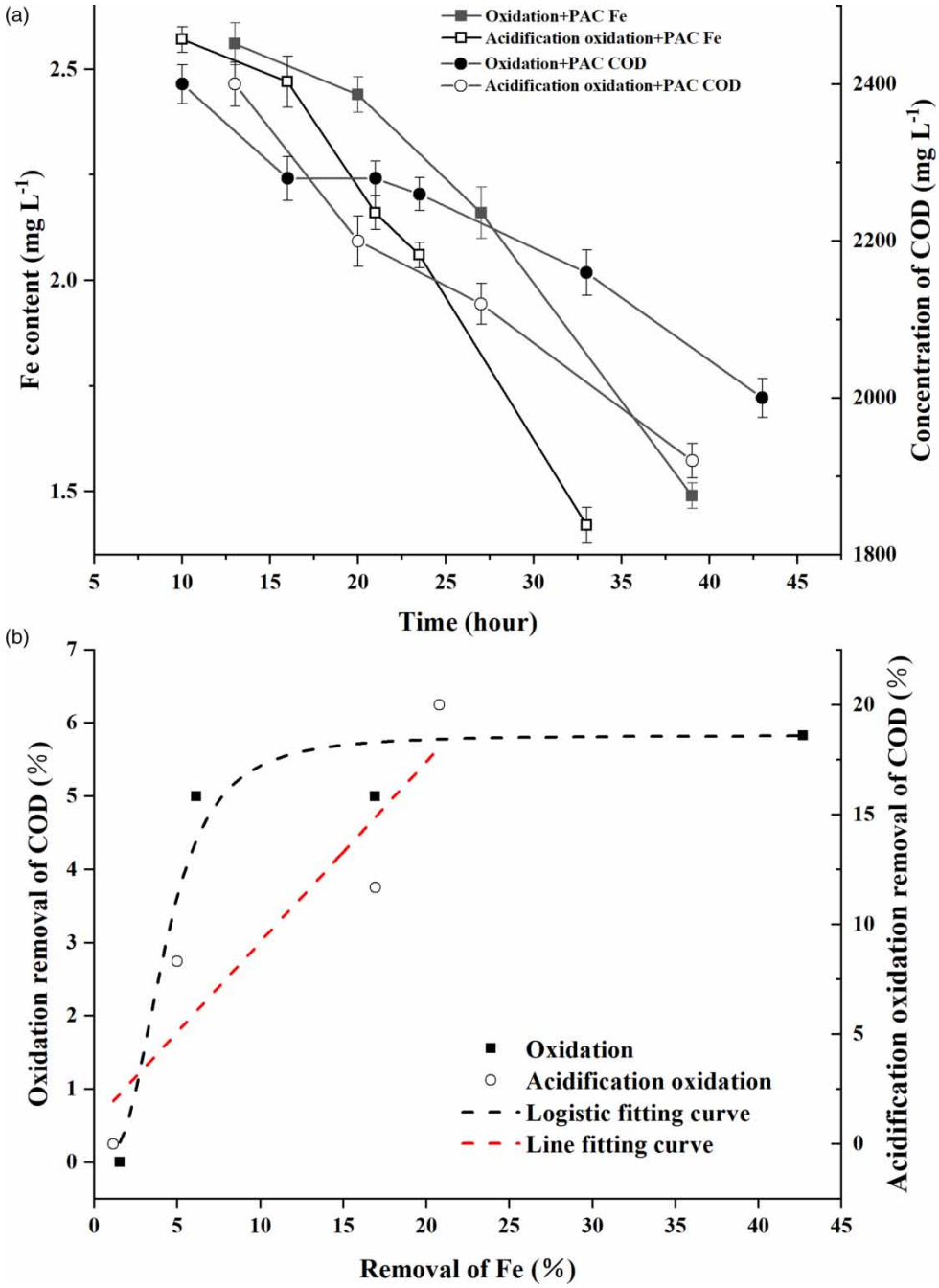


**Figure 8** | Effect of acidification oxidation and direct oxidation on COD and Fe removal over time (a) and their correlation (b).

development of the novel demulsification–oxidation–coagulation technique. Based on the observed floc structure, the orange-red dyed oil droplets of $NaClO_x + CaO + PAC$ interacted with the oil more strongly than $NaClO_x + CaO$ or pure PAC. $Ca^{2+}$ exhibited a better demulsification effect than $Na^{+}$, with the corresponding oil removal rate increasing from 72 to 83%. Because the iron removal efficiency is related to the pH, CaO addition was more advantageous. Oil removal is related to the exothermic heat generated by reagent hydration, so it is more advantageous to add $Ca(OH)_2$. From the FTIR analysis, the oil wastewater contained many hydrophobic alkanes. In the $NaClO_x + CaO + PAC$ process, the alkanes were converted into hydrophilic alcohols and aldehydes, forming ferrous iron hydroxides that can be used as flocs, thereby increasing the oil removal rate. The best performance was achieved with 400 μL of $NaClO_x$, 200 μL of 1 mol $L^{-1}$ CaO, and 12 mL of 12.8 g $L^{-1}$

PAC. Furthermore, the combination of acidification and oxidation was more efficient than direct oxidation for removing Fe and COD.

In future field applications, mechanically washed wastewater will be initially acidified. Adding CaO to demulsify, combined with $NaClO_x$ oxidation, destroys the water-in-oil structure and rapidly changes the environmental fate of $Fe^{2+}$ to $Fe(OH)_3$, thereby improving overall oil and iron removal efficiency.

## ACKNOWLEDGEMENTS

This work was financially supported by the Natural Science Foundation of China (Grant No. 51808044), the Natural Science Foundation of Shaan Xi Province of China (Grant No. 2020JM-262), Shendong Coal Branch Technology Innovation Project of China Shenhua Energy Co., Ltd (Grant No. CEZB210304069), and the Fundamental Research Funds for the Central Universities, CHD (Grant No. 300102281502).

## AUTHOR CONTRIBUTIONS

J.Q.: Conceptualization; Methodology; Supervision; Y.H.: Methodology; Writing – Original Draft; B.S.: Formal analysis; Validation; R.W.: Data Curation; Investigation; X.W.: Resources; Project administration; C.Q.: Resources; Project administration; Y.W.: Resources; Project administration.

## DATA AVAILABILITY STATEMENT

All relevant data are included in the paper or its Supplementary Information.

## CONFLICT OF INTEREST

The authors declare there is no conflict.

## REFERENCES

Atesok, G., Somasundaran, P. & Morgan, L. J. 1988 Adsorption properties of $Ca^{2+}$ on Na-kaolinite and its effect on flocculation using polyacrylamides. *Colloids and Surfaces* **32** (1–2), 127–138. https://doi.org/10.1016/0166-6622(88)80009-X.

Cañizares, P., Jiménez, C., Martínez, F., Sáez, C. & Rodrigo, M. A. 2007 Study of the electrocoagulation process using aluminum and iron electrodes. *Industrial and Engineering Chemistry Research* **46** (19), 6189–6195.

Cao, S., Jiang, W., Zhao, M., Liu, A., Wang, M., Wu, Q. & Sun, Y. 2018 Green synthesis of amphipathic graphene aerogel constructed by using the framework of polymer-surfactant complex for water remediation. *Applied Surface Science* **444** (June 30), 399–406. https://doi.org/10.1016/j.apsusc.2018.02.282.

Chaprão, M. J. S., de Cassia Freire Soares Rufino, R., Luna, R. D., Santos, J. M., Sarubbo, V. A. & Asfora, L. 2018 Formulation and application of a biosurfactant from *Bacillus methylotrophicus* as collector in the flotation of oily water in industrial environment. *Journal of Biotechnology* **285**, 15–22. https://doi.org/10.1016/j.jbiotec.2018.08.016.

Chen, L., Ye, F., Liu, H., Jiang, X., Zhao, Q., Ai, G., Shen, L., Feng, X., Yang, Y. & Mi, Y. J. C. 2022 Demulsification of oily wastewater using a nano carbon black modified with polyethyleneimine. (May): 295. F.N. Crespilho and M. Rezende, *Eletroflotação – Princípios e Aplicações*.

Crespilho, F. N. & Rezende, M. O. O. 2004 *Eletroflotação: Princípios e Aplicações*, 1st ed., Editora Rima, São Carlos, Brazil.

Darvishmotevalli, M., Zarei, A., Moradnia, M., Noorisepehr, M. & Mohammadi, H. 2019 Optimization of saline wastewater treatment using electrochemical oxidation process: prediction by RSM method. *MethodsX* **6**, 1101–1113.

Deghles, A. & Kurt, U. 2016 Treatment of tannery wastewater by a hybrid electrocoagulation/electrodialysis process. *Chemical Engineering and Processing: Process Intensification* **104**, 43–50.

Deng, W., Dai, Q. & Lao, Y., Shi, B. & Wang, X. 2016 Low temperature catalytic combustion of 1, 2-dichlorobenzene over $CeO_2$–$TiO_2$ mixed oxide catalysts. *Applied Catalysis B: Environmental* **181**, 848–861.

Fard, A. K., Rhadfi, T., Mckay, G., Al-Marri, M. & A., M. 2016 Enhancing oil removal from water using ferric oxide nanoparticles doped carbon nanotubes adsorbents. *Chemical Engineering Journal* **293**, 90–101. https://doi.org/ 10.1016/j.cej.2016.02.040.

Ganiyu, S. O., Martinez-Hutile, C. A. & Oturan, M. A. 2020 Electrochemical advanced oxidation processes for wastewater treatment: advances in formation and detection of reactive species and mechanisms. *Current Opinion in Electrochemistry* **27**, 100678.

Han, M., Zhang, J. & Chu, W., Chen, J. & Zhou, G. 2019 Research progress and prospects of marine oily wastewater treatment: a review. *Water* **11** (12), 2517.

Hodaifa, G., Gallardo, P. A., García, C. A., Kowalska, M. A. & Seyedsalehi, M. 2019 Chemical oxidation methods for treatment of real industrial olive oil mill wastewater. *Journal of the Taiwan Institute of Chemical Engineers* **97**, 247–254.

Hui, L., Yan, W., Juan, W. & Zhongming, L. 2015 A review: recent advances in oily wastewater treatment. *Recent Patents on Chemical Engineering* **7** (1), 17–24. https://doi.org/10.1016/j.toxlet.2010.12.010.

Iskandar, M. J., Baharum, A. & Anuar, F. H. & Othaman, R. 2018 Palm oil industry in South East Asia and the effluent treatment technology – a review. *Environmental Technology & Innovation* **9**, 169–185. https://doi.org/10.1016/j.eti.2017.11.003.

Kim, S. H., Moon, B. H. & Lee, H. I. 2001 Effects of pH and dosage on pollutant removal and floc structure during coagulation. *Microchemical Journal* **68** (2–3), 197–203. https://doi.org/10.2174/2211334707666140415222545.

Lee, K. E., Morad, N., Teng, T. T. & Poh, B. 2012 Development, characterization and the application of hybrid materials in coagulation/flocculation of wastewater: A review. *Chemical Engineering Journal* **203**, 370–386.

Liu, G., Du, C. & Xie, X. 2020 Application of double filtration technology in pretreatment of emulsion wastewater and cleaning wastewater in machining industry. *Modern Industrial Economy and Informationization* 10, 197(11), 63–65.

Lv, M., Zhang, Z., Zeng, J., Liu, J., Sun, M., Yadav, R. & Feng, Y. 2018 Roles of magnetic particles in magnetic seeding coagulation-flocculation process for surface water treatment. *Separation and Purification Technology* **212**, 337–343.

Meng, J. L., Zhang, R. B., Zhang, Z. Y., Jia, L. Y. & Pang, W. L. 2012 Oil separation/sedimentation/air floatation/biochemical process for treatment of wastewater from machining park. *China Water & Wastewater* **28** (8), 39–41.

Moussa, D. T., El-Naas, M. H., Nasser, M. & Al-Marri, M. J. 2017 A comprehensive review of electrocoagulation for water treatment: potentials and challenges. *Journal of Environmental Management* **186** (pt.1), 24–41.

Munirasu, S., Haija, M. A. & Banat, F. 2016 Use of membrane technology for oil field and refinery produced water treatment – a review[J]. *Process Safety and Environmental Protection* **100**, 183–202.

Pardo, P., Anxionnaz-Minvielle, Z., Rouge, S., Cognet, P. & Cabassud, M. J. S. E. 2014 Ca(OH)2/CaO reversible reaction in a fluidized bed reactor for thermochemical heat storage. **107** (Sep), 605–616.

Qin, J., Gong, Y., Qin, C., Meng, H. & Gao, J. 2021 CO2 introduced the coagulation-flocculation of oil acidized wastewater: pollutant removal and cost analysis. *Water Science & Technology* **83** (3), 1108–1117.

Rohman, A. & Man, Y. 2010 Fourier transform infrared (FTIR) spectroscopy for analysis of extra virgin olive oil adulterated with palm oil. *Food Research International* **43** (3), 886–892.

Simate, G. S., Iyuke, S. E., Ndlovu, S. & Heydenrych, M. 2015 The heterogeneous coagulation and flocculation of brewery wastewater using carbon nanotubes. *Water Research* **21** (4), 1277–1285.

Sillanpää, M., Ncibi, M. C., Matilainen, A. & Vepsalainen, M. 2018 Removal of natural organic matter in drinking water treatment by coagulation: a comprehensive review. *Chemosphere* **190** (Jan), 54.

Sun, Y., Zhu, C., Zheng, H., Sun, W. J., Xu, Y., Xuefeng, X., You, Z. & Cuiyun, L. 2017 Characterization and coagulation behavior of polymeric aluminum ferric silicate for high-concentration oily wastewater treatment. *Chemical Engineering Research & Design* **119**, 23–32.

Voort, F., Ismail, A. A., Sedman, J. & Emo, G. 1994 Monitoring the oxidation of edible oils by Fourier transform infrared spectroscopy. *Journal of the American Oil Chemists Society* **71** (3), 243–253.

Wang, X., Liang, L. & Xie, J. 2006 Research on the treatment of wastewater from oil production by flocculation sedimentation - NaClO/activated carbon oxidation–adsorption. *Industrial Water Treatment* **2006** (12), 60–62. https://doi.org/10.1016/S1872-2040(06)60041-8.

Wong, S. F., Lim, J. S. & Dol, S. S. 2015 Crude oil emulsion: A review on formation, classification and stability of water-in-oil emulsions[J]. *Journal of Petroleum Science and Engineering* **135**, 498–504.

Wen, X., Du, C., Zeng, G., Huang, D., Zhang, J., Yin, L., Tan, S., Huang, L., Chen, H. & Yu, G. 2018 A novel biosorbent prepared by immobilized *Bacillus licheniformis* for lead removal from wastewater. *Chemosphere* **200** (June), 173–179.

Xiao, Y., De Araujo, C., Sze, C. C. & Stuckey, D. C. 2015 Toxicity measurement in biological wastewater treatment processes: a review. *Journal of Hazardous Materials* **286**, 15–29. https://doi.org/10.1016/j.jhazmat.2014.12.033.

Yalcinkaya, F., Boyraz, E., Maryska, J. & Kucerova, K. 2020 A review on membrane technology and chemical surface modification for the oily wastewater treatment. *Industrial and Organizational Psychology* **13** (2), 493.

Yan, M., Wang, D., Ni, J., Qu, J., Chow, C. W. & Liu, H. 2008 Mechanism of natural organic matter removal by polyaluminum chloride: effect of coagulant particle size and hydrolysis kinetics. *Water Research* **42** (13), 3361–3370. https://doi.org/10.1016/j.watres.2008.04.017.

You, Z., Xu, H., Sun, Y., Zhang, S. & Zhang, L. 2018 Effective treatment of emulsified oil wastewater by the coagulation–flotation process. *RSC Advances* **8** (71), 40639–40646.

Zhao, X., Liu, L., Wang, Y., Dai, H., Wang, D. & Cai, H. 2008 Influences of partially hydrolyzed polyacrylamide (hpam) residue on the flocculation behavior of oily wastewater produced from polymer flooding. *Separation & Purification Technology* **62** (1), 199–204.

Zeng, Y., Yang, C., Zhang, J. & Pu, W. 2007 Feasibility investigation of oily wastewater treatment by combination of zinc and pam in coagulation/flocculation. *Journal of Hazardous Materials* **147** (3), 991–996.

Zhang, W., Na, L., Cao, Y., Xin, L. & Lin, F. 2017 Superwetting porous materials for wastewater treatment: from immiscible oil/water mixture to emulsion separation. *Advanced Materials Interfaces* **4** (10), 1600029.

Zhang, Q., Yu, Z. & Cheng, W. N. 2015 Wastewater monitoring program for environmental protection in papermaking industry for check and accept of completed construction project. *Paper Science & Technology* **34** (4), 89–91.

Zheng, H., Gao, Y., Cai, L., Liu, B., Hou, J., Huang, W. & Zhou, Y. 2015 Research and development status of poly aluminum chloride coagulant. *Inorganic Chemicals Industry* **26** (12), 62–90.

First received 18 September 2022; accepted in revised form 16 January 2023. Available online 1 February 2023